IOP Conf. Series: Materials Science and Engineering **330** (2018) 012015 doi:10.1088/1757-899X/330/1/012015

Effect of Microstructure on Stress Corrosion Cracking Behaviour of High Nitrogen Stainless Steel Gas Tungsten Arc Welds

Raffi Mohammed[1*], Srinivasa Rao K[2], Madhusudhan Reddy G[3]
[1]Department of Metallurgical & Materials Engineering, NIT - Andhra Pradesh, India
[2]Department of Metallurgical Engineering, Andhra University, Visakhapatnam, India
[3]Defence Metallurgical Research Laboratory, Hyderabad, India

*Corresponding author E-mail: raffia.u@gmail.com

Abstract. Present work is aimed to improve stress corrosion cracking resistance of high nitrogen steel and its welds. An attempt to weld high nitrogen steel of 5 mm thick plate using gas tungsten arc welding (GTAW) with three high strength age hardenable fillers i.e., 11-10 PH filler, PH 13-8Mo and maraging grade of MDN 250 filler is made. Welds were characterized by optical microscopy and scanning electron microscopy. Vickers hardness testing of the welds was carried out to study the mechanical behaviour of welds. Potentio-dynamic polarization studies were done to determine pitting corrosion resistance in aerated 3.5% NaCl solution. Stress corrosion cracking (SCC) testing was carried out using constant load type machine with applied stress of 50% yield strength and in 45% $MgCl_2$ solution boiling at 155°C. The results of the present investigation established that improvement in resistance to stress corrosion cracking was observed for PH 13-8Mo GTA welds when compared to 11-10 PH and MDN 250 GTA welds. However, All GTA welds failed in the weld interface region. This may be attributed to relatively lower pitting potential in weld interface which acts as active site and the initiation source of pitting.

1. Introduction

Stainless steels are known for structural application due to better combination of strength and corrosion resistance. Typically austenitic stainless steel requires a combination of 8% Nickel (Ni) and 18% Chromium (Cr) to achieve required strength and corrosion resistance [1]. Even though conventional stainless steels are fully austenitic, they are generally not considered because of higher cost associated with high Ni content. However, replacing carbon (C) in stainless steel with nitrogen (N) became favorable since N is a strong austenite stabilizer, and has greater solubility than C [2]. An austenitic material generally is considered high-N if it contains > 0.4 wt% N [3]. High nitrogen steels have much higher yield strength than the 300 grade steels such as 304 and 316 stainless steels [4-7]. High nitrogen austenitic stainless steel is a nickel free high Cr-Mn-N steel having a wide scope in the defense sector for manufacturing battle tanks with an aim to replace the existing armor steel. High nitrogen steels (HNS) are becoming an important engineering material with an excellent combination of superior strength, toughness and wear resistance [8]. Nitrogen effectively acts as a solid solution strengthener than carbon and enhances grain size strengthening [9, 10]. High nitrogen in solid solution is a beneficial alloying element to raise the strength without drop in ductility and toughness. Nitrogen is a very good austenite stabilizer and reduces the amount of nickel for stabilizing austenite. It also remarkably improves resistance to intergranular, pitting, crevice and stress corrosion cracking [11]. Even though base metal exhibits better combination of properties, welding may result in significant loss of mechanical properties and corrosion

resistance. In the conventional fusion welding process, severe problems like nitrogen induced porosity, solidification cracking in the weld zone, nitrogen desorption, lowering the dissolved nitrogen for solute strengthening and Cr-nitrides precipitation in the heat affected zone was observed [12]. Welding requires special care to ensure that the nitrogen remains in the weld metal due to high nitrogen content. Proper selection of filler metal is important to overcome the above problems and should be aimed at low impurity levels and good control on segregation of alloying elements [13]. If the solubility limit of nitrogen level during or prior to solidification in welding, leads to the formation of nitrogen bubbles and thereby increasing the likelihood for nitrogen induced porosity [14]. Using matching filler wire of similar composition or by choosing a filler wire may overcome solidification cracking which produces enough amount of delta ferrite in fusion welds. Based on service performance, requirement of delta ferrite in austenitic stainless steel welds is often specified to ensure that weld metal may relieve the cracking tendency [15]. Reducing the inter-metallic precipitation compounds by raising the austenite/ferrite transformation temperature in the heat affected zone is achieved by nitrogen alloying [16]. Presently no matching filler wires are commercially available for welding high nitrogen austenitic stainless steel. Existing literature related to welding of nickel free high nitrogen stainless steel (HNS) is scarce. The present study assumes significance since systematic approach on studies related to microstructural changes and its correlation with mechanical and corrosion behaviour of nickel free high nitrogen stainless steel and its welds have not been reported so far in the literature. In view of the above facts, the present work has been aimed to improve the corrosion resistance along with mechanical properties of the welds of nickel free high nitrogen stainless steel by controlling the microstructural changes during gas tungsten arc welding.

2. Experimental Details

Nickel free high nitrogen steel (HNS) plates of size (500mmx150mmx5mm) in wrought form were used in the present study and the GTA welds made with various filler wires were carried out. The base metal and filler wires compositions were given in the Table 1 and 2. After having several experiments, welding parameters were optimized and obtained a sound welds free from defects are shown in Fig.1. Optimized welding parameters of all the welding processes are given in the Table 3. Microstructural studies were characterized at various zones of the welds using optical microscopy and scanning electron microscopy. Microhardness values were recorded towards the longitudinal directions of the weld with a load of 0.5Kgf for 20 seconds as per ASTM E384-09 standards using Vickers hardness testing machine. Pitting corrosion resistance of welds was determined using potentio-dynamic polarization testing in 3.5%NaCl solution. Flat tensile specimens for SCC were prepared as per ASTM E8 standards. Stress corrosion cracking (SCC) testing was carried out using constant load type machine with applied stress of 50% yield strength and in 45% $MgCl_2$ solution boiling at 155°C as per ASTM G36 standards.

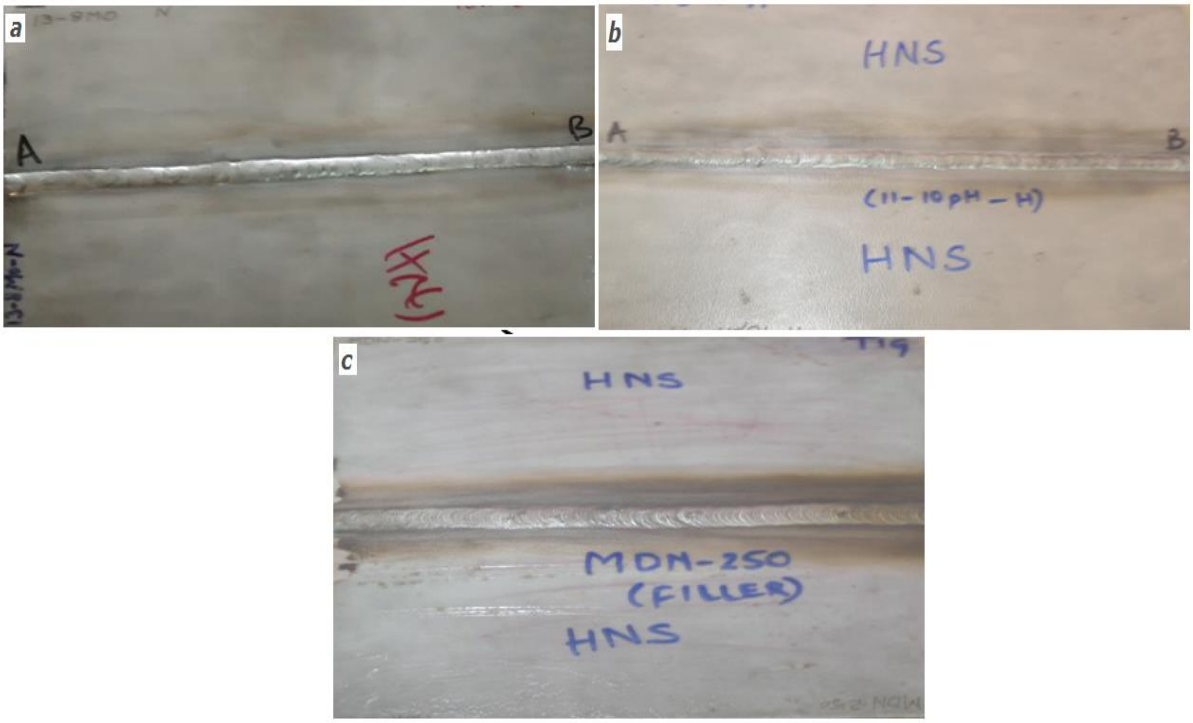

Fig. 1 HNS weldments made of (a).PH 13-8Mo filler; (b). 11-10 PH filler and (c). MDN 250 filler

Table 1 Nominal chemical composition of the base material

Material	Element (wt %)										
	C	Mn	Cr	N	S	P	Ni	Co	Mo	Si	Fe
HNS	0.076	19.78	17.96	0.543	0.007	0.051	-	-	-	0.34	Bal.

Table 2 Chemical composition of the filler wires

Material	Element (wt %)										
	C	Mn	Cr	N	S	P	Ni	Co	Mo	Si	Fe
11-10 PH	0.07	1.00	11	-	0.030	0.040	10	-	-	1.00	Bal.
MDN 250	0.03	0.10	0.50	-	0.10	0.01	18	8	-	0.10	Bal.
H 13-8Mo	0.05	-	13.25	-	-	-	8.50	-	2.50	-	Bal.

Table 3 Welding parameters using Gas Tungsten Arc Welding

Welding Current (A)	130
Welding Speed (mm/sec)	60
Electrode polarity	DCSP
Arc voltage (V)	18-20
Filler wire diameter (mm)	1.6
Electrode	2% thoriated tungsten
No. of passes	2
Shielding gas	Argon

3. Results and discussion

3.1. Microstructure

3.1.1. Nickel free high nitrogen steel. Fine grains of austenite and annealing austenite twins are observed in the optical and scanning electron micrographs of the base metal and are shown in Fig. 2. In high nitrogen steel, nitrogen acts as austenite stabilizer and effective in completely replacing nickel. Addition of chromium and manganese increase the solubility of nitrogen. Therefore, nitrogen content in Fe-Cr-Ni alloys are much lower than that in Fe-Cr-Mn alloys and other alloying elements like Ti, V, Nb and Zr enhance the solubility due to their high affinity for nitrogen. In the present investigation, three fillers 11-10 PH, MDN 250 and PH 13-8 Mo are selected with an aim to achieve better combination of mechanical and corrosion properties of high nitrogen steel welds.

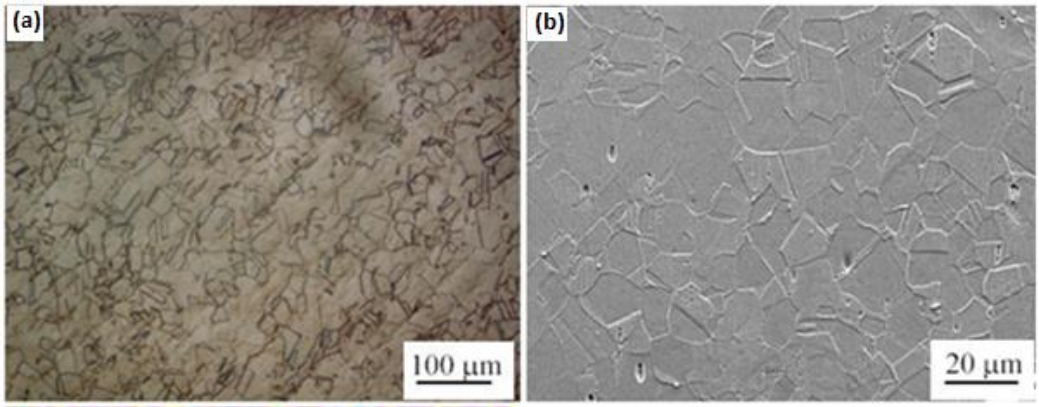

Fig. 2 Micrograph of base metal (high nitrogen stainless steel) (a) optical (b) scanning electron micrograph

3.1.2. Gas tungsten arc welds. Fig. 3 shows the optical and scanning electron micrographs of weld zone for the high nitrogen steel welds made with age hardenable 11-10 PH filler. Weld microstructure is observed to have the network of fine dispersed delta ferrite in the austenite matrix. After complete cooling

and solidification of the weld microstructure depends upon the quantity of ferrite which existed at very high temperature and consequently upon the relative proportions of austenite and ferrite formers.

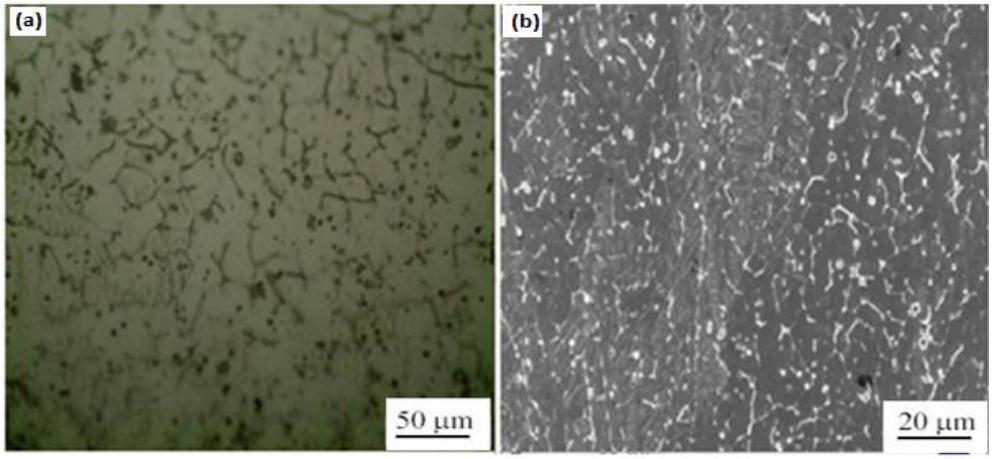

Fig. 3 Micrographs of weld zone of 11-10 PH GTA weld of high nitrogen stainless steel (a) Optical and (b) SEM

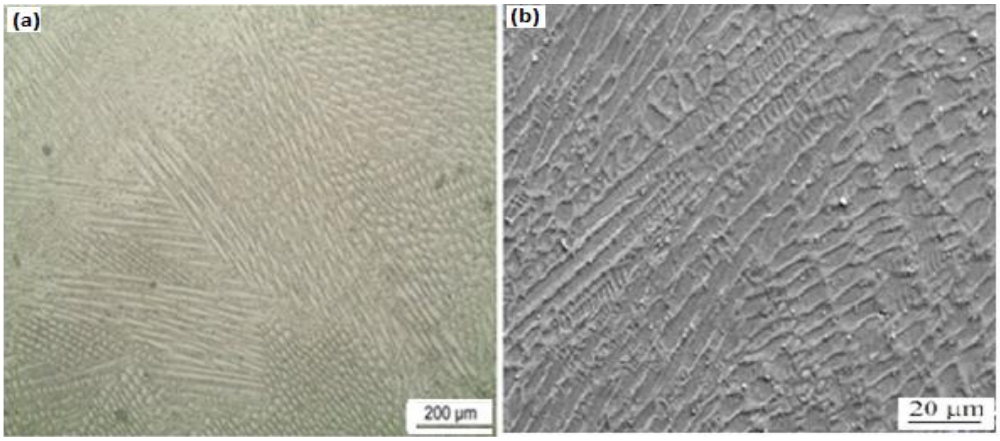

Fig. 4 Micrographs of weld zone of MDN 250 GTA weld of high nitrogen stainless steel (a) Optical and (b) SEM

Fig. 4 shows the optical and scanning electron micrograph of weld zone for the GTA welds made with MDN 250 maraging steel. Island pool of reverted austenite in the martensite matrix was observed [21]. Fig. 5 shows the optical and scanning electron micrograph of weld zone for the GTA welds made with high strength and corrosion resistant age hardenable PH 13-8Mo filler. Delta ferrite of the discontinuous network in the austenite matrix is observed in the weld metal and relatively fine grains may be due to the presence of Mo which is a strong ferrite stabilizer.

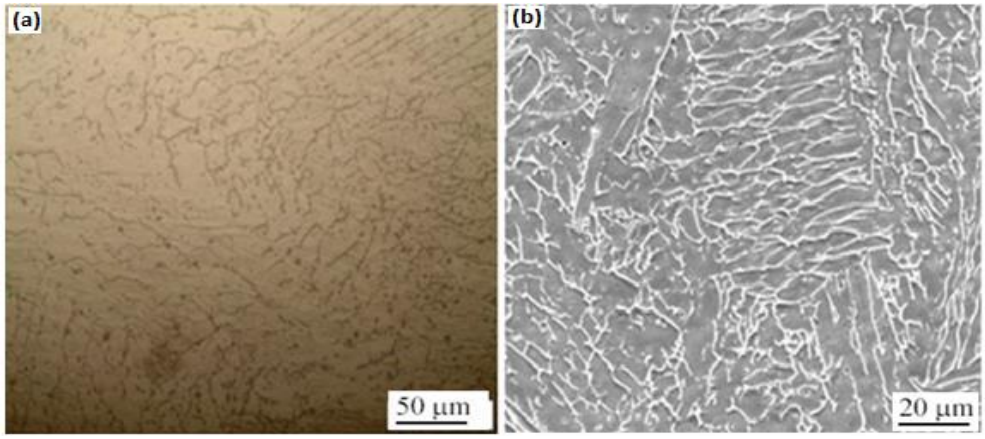

Fig. 5 Micrographs of weld zone of PH 13-8Mo GTA weld of high nitrogen stainless steel (a) Optical and (b) SEM

Fig 6 shows the optical and SEM micrograph of the weld interface for 11-10 PH GTA welds. It is clearly evident that in the weld interface along the fusion boundary, micropores were observed in the partially melted zone towards the base metal. Partially melted zone next to the fusion boundary resulted in having nitrogen content significantly higher than the solubility of nitrogen in the liquid metal. Pores are formed due to entrapment of nitrogen in partially melted zone [22].

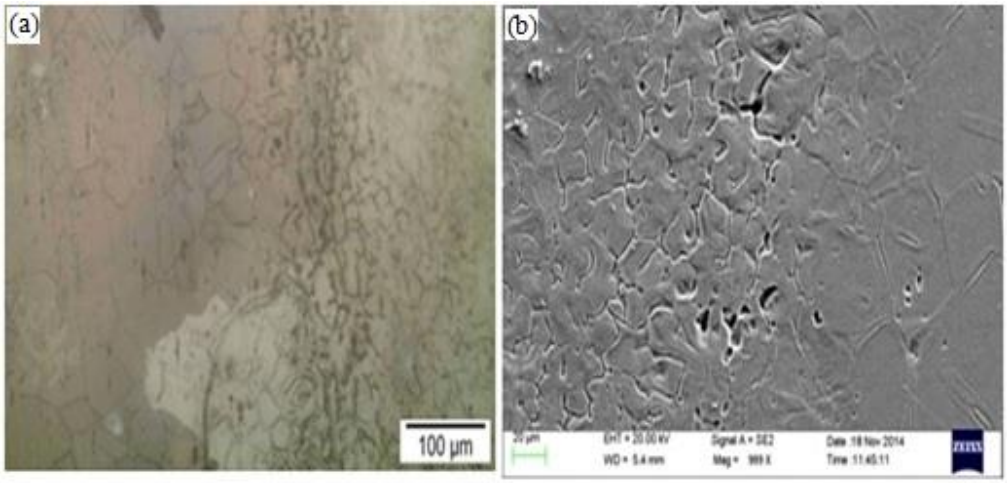

Fig. 6 Micrographs of weld interface of 11-10 PH GTA weld of high nitrogen stainless steel (a) Optical and (b) SEM

Fig. 7 shows the optical and SEM micrograph of the weld interface for MDN 250 GTA weld. In the weld metal for the GTA welds made with maraging grade of MDN 250 filler, elongated austenite island pools in the martensite matrix were observed. In the weld interface, it is observed the formation of a thin layer of unmixed zone adjacent to the fusion line. The unmixed zone is the region where the base metal that was melted, but do not mix with the filler metal.

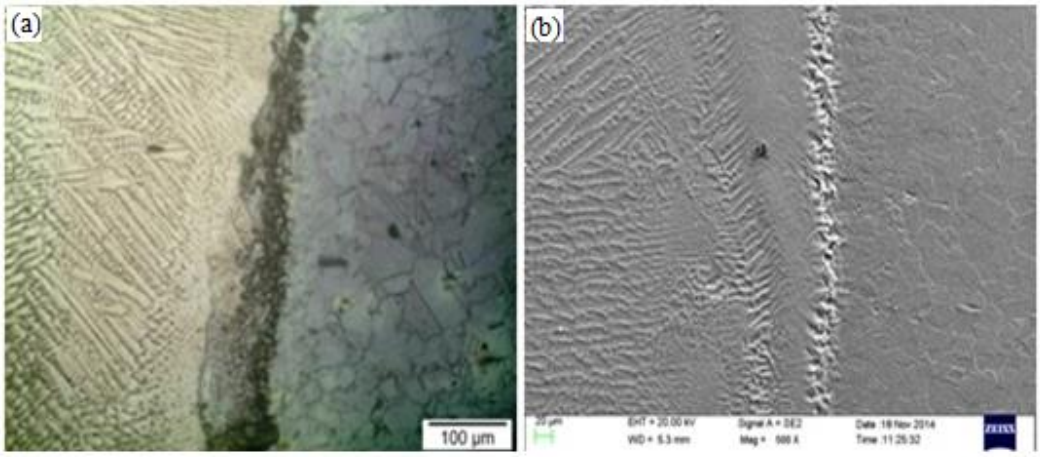

Fig. 7 Micrographs of weld interface of MDN 250 GTA weld of high nitrogen stainless steel (a) Optical and (b) SEM

Fig. 8 shows optical and SEM micrograph of weld interface for PH 13-8Mo GTA welds. It is clearly evident that the weld metal microstructure is having delta ferrite discontinuous network in the austenite matrix. In weld interface, no significant porosity was observed and is due to the maximum dilution of weld metal to the adjacent base metal.

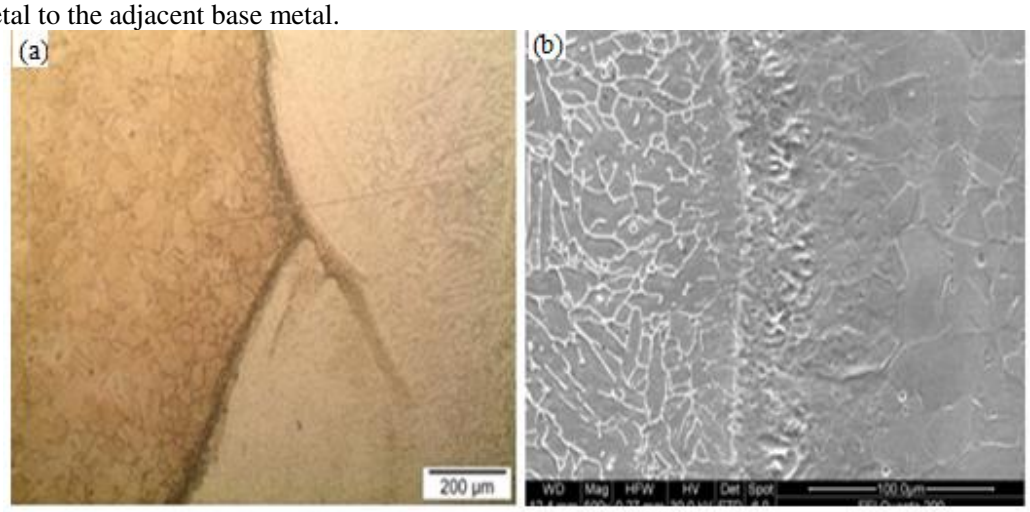

Fig. 8 Micrographs of weld interface of PH13-8Mo GTA weld of high nitrogen stainless steel (a) Optical and (b) SEM

PH 13-8 Mo GTA welds are having relatively fine grains and discontinuous delta ferrite distribution in the austenite matrix in the weld metal. The weld interface of PH 13-8 Mo GTA welds is free from porosity and unmixed zone when compared to that of 11-10 PH and MDN 250 GTA welds.

3.2. Mechanical properties

Fig. 9 shows the hardness survey for GTA welds made with three fillers viz., 11-10 PH, MDN 250 and 13-8Mo fillers. Hardness survey covers fusion zone, weld interface, heat affected zone and the base metal. The Vickers hardness value of the base metal is observed as 410 VHN whereas the hardness values are

observed to be lower in the weld zone than the base metal for all the three welds. Welds made with 11-10 PH filler are having weld zone hardness value of 240 VHN, MDN 250 filler is having weld zone hardness value of 211 VHN and 13-8Mo PH filler is having 270 VHN in the weld zone. Reduction in hardness value of weld zones is attributed to changes in microstructure, chemical composition and relative coarse grains formed in the welds when compared to a base metal. From the hardness survey of all the three welds, similar behaviour of having lower strength in the fusion zone was exhibited. Again the hardness is improved from the weld interface towards the base metal. From Fig. 9 it is clearly evident that GTA weld made with 13-8Mo filler is observed to be having a higher hardness when compared to welds made with 11-10PH and MDN 250 filler. Tensile testing for high nitrogen steel and its welds are observed to fail at the weld zone due to poor hardness and it can be seen in Fig.9 and given in Table 4.

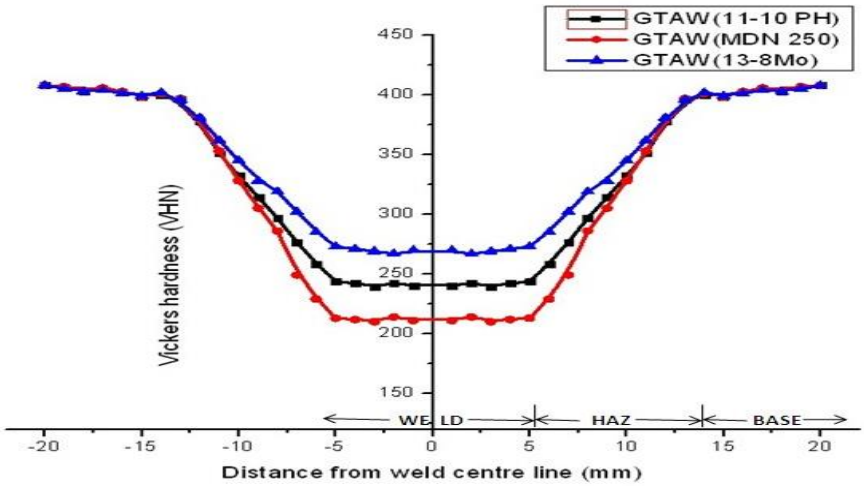

Fig. 9 Vickers hardness survey of gas tungsten arc welds of high nitrogen stainless steel

Table 4 Tensile values of nickel free high Cr-Mn-N steel welds

Material	UTS (MPa)	Y S (MPa)	% E l	Location of Failure
HNS Base	1215	1190	22	Base
SMAW (Cr-Mn-N)	667	233	10	Weld
GTAW (MDN 250)	919	644	9.2	Weld
EBW	1065	811	5.8	Weld

3.3. Pitting corrosion

Potentio-dynamic polarization curve of the base metal in 3.5% NaCl solution and the pitting potential (Epit) is found to be 130mV. As the morphology of the base metal is having a single austenite phase, homogenous and fine grain size, formation of compact passive film is easy and difficult for chloride ion to penetrate through thus the corrosion resistance of the base material is better. Role of nitrogen in improving the pitting corrosion resistance is due to the formation of ammonium ions enriched at passive film/ pit site acts as an inhibitor and thus retards the pit growth [19]. Figs. 10– 13 shows the potentio-dynamic

polarization curves for GTA welds made with 11-10 PH filler, MDN 250 filler and 13-8Mo filler. Each weldment was tested in three distinct regions of weld zone, weld interface (PMZ/HAZ) and base metal. Fig. 10 shows the potentio-dynamic polarization curves for GTA welds made with 11-10 PH filler. Weld zone of GTA welds made with 11-10 PH filler exhibited critical pitting potential (Epit) of 115mV when compared to base metal of 130mV. Whereas weld interface assumed to be either PMZ/HAZ is having relatively much lower critical pitting potential (Epit) of -55mV which may become anodic to weld zone and base metal. Hence, preferential attack may initiate at the weld interface when compared to weld zone and base metal.

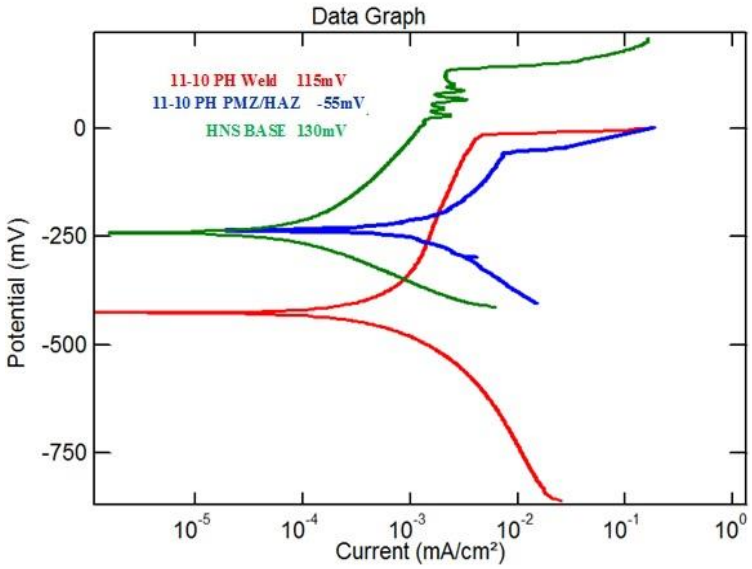

Fig. 10 Potentio-dynamic polarization curves of 11-10 PH GTA welds of high nitrogen stainless steel

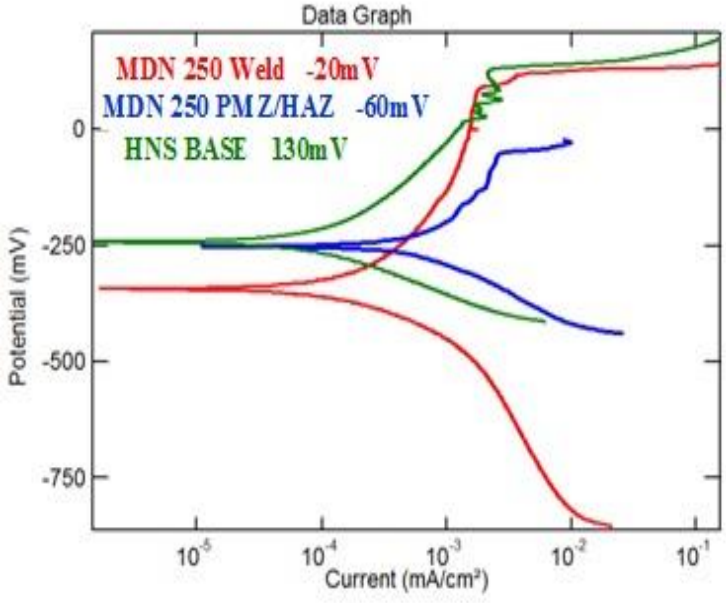

Fig. 11 Potentio-dynamic polarization curves of MDN 250 GTA welds of high nitrogen stainless steel

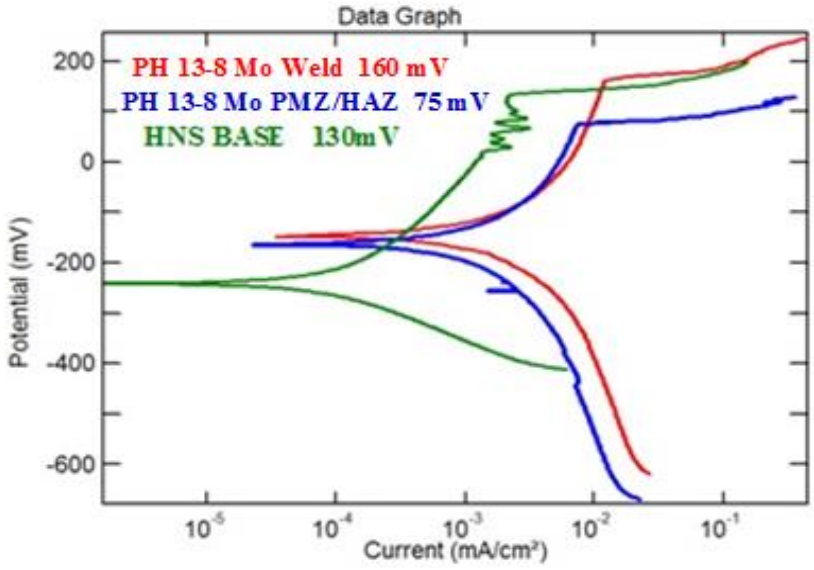

Fig. 12 Potentio-dynamic polarization curves of PH 13-8Mo GTA welds of high nitrogen stainless steel

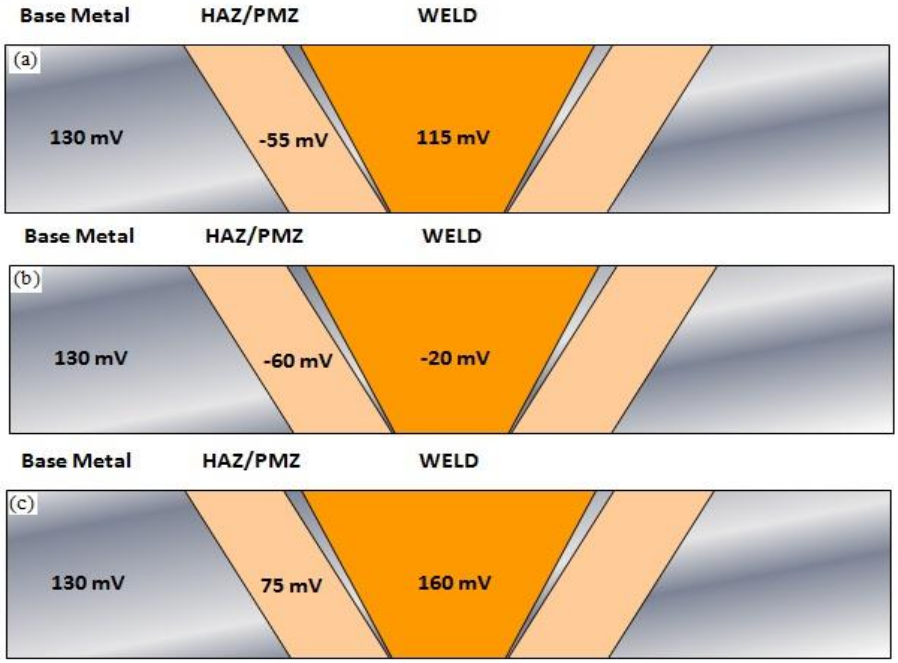

Fig. 13 Pitting potential values of GTA welds of high nitrogen stainless steel made with (a) 11-10PH filler (b) MDN 250 filler and PH 13-8Mo filler

Fig. 11 shows the potentio-dynamic polarization curves of MDN 250 GTA welds. Pitting potential (Epit) of weld zone is found to be -20mV, weld interface exhibited -60mV and base metal having 130mV. Weld

interface acts as anodic due to relatively more negative pitting potential. Pit initiates in this region and grows rapidly when compared to weld zone and the base metal. Fig. 12 shows the potentio-dynamic polarization curves for GTA welds made with PH 13-8 Mo filler. In PH 13-8 Mo GTA welds, pitting potential (Epit) is found to be 160mV in the weld zone, 75mV in the weld interface and 130mV in the base metal. As the weld interface is observed to have relatively more negative, pitting potential (Epit) value and becomes anodic when compared to weld zone and base metal. Fig. 13 shows the pitting potential values in different regions of the GTA welds. In all the three welds, pitting corrosion initiates at the weld interface as it is having lower pitting potential compared to weld zone and base metal. Relatively higher film stability is observed in the welds made with 13-8Mo filler and is attributed to the presence of molybdenum and grain refinement. Hence, PH 13-8 Mo GTA welds are having higher pitting corrosion resistance when compared to 11-10 PH and MDN 250 GTA welds.

3.4. Stress corrosion cracking

Stress corrosion cracking testing was carried out with a constant load SCC machine with a fabricated cell. Tensile specimens were loaded with 50% yield stress of the material and tested in a more aggressive environment of 45% $MgCl_2$ solution boiling at 155°C. The failed test specimen is shown in Fig. 14a and stress-time curve is given in Fig. 14b. Failure time was found to be 25 hours and given in Table 5. SEM fractograph is as shown in Fig. 13c and it clearly reveals the mixed mode of failure with multiple cracks and is an evidence of both intergranular and transgranular stress corrosion cracking mechanisms. Hence the base metal (HNS) is susceptible to SCC in a test environment. SCC failed test specimen of 11-10 PH GTA weld is shown in Fig. 15a and stress-time curve is given in Fig. 15b. Failure time is found to be 16 hours. Fractograph as shown in Fig. 15c and it clearly reveals the attack in the weld interface region. SCC test data is given in Table 5. Failure can be correlated to observed microstructural changes and microporosity in the weld interface. Weld interface is susceptible to pitting and stress corrosion cracking and is attributed to microporosity. Porosity may lead to faster initiation of pitting attack since this region acts as active sites for stress concentration [23].

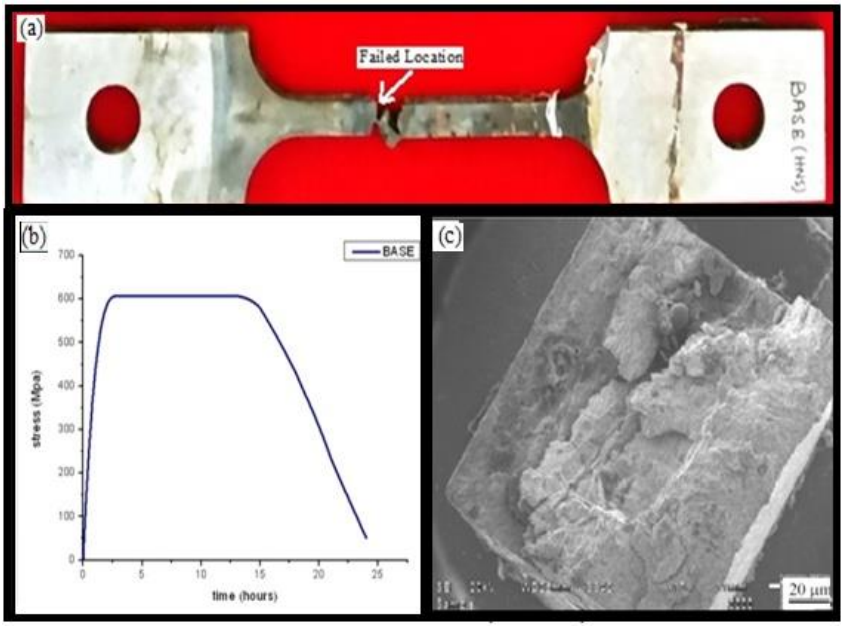

Fig. 14 Stress corrosion cracking test specimen of high nitrogen stainless steel (a) failed SCC specimen (b) stress-time curve and (c) SEM fractograph

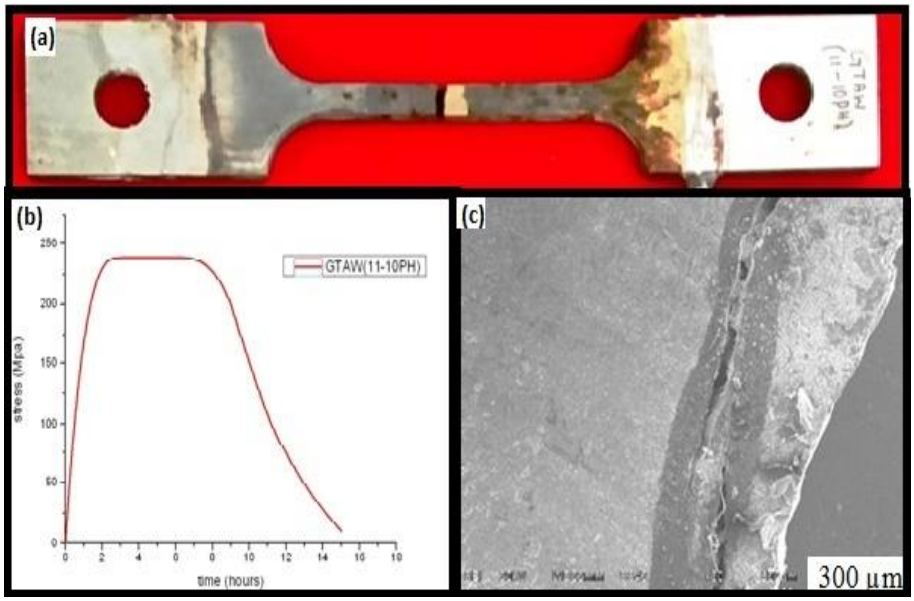

Fig. 15 Stress corrosion cracking specimen of 11-10 PH GTA welds of high nitrogen stainless steel (a) failed SCC specimen (b) stress- time curve and (c) SEM fractograph

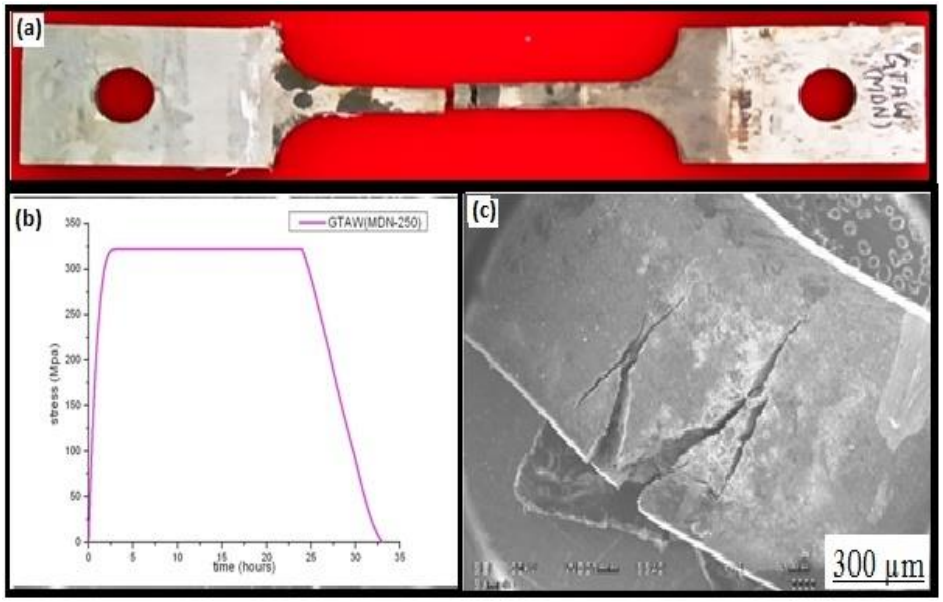

Fig. 16 Stress corrosion cracking specimen of MDN 250 GTA welds of high nitrogen stainless steel (a) failed SCC specimen (b) stress-time curve and (c) SEM fractograph

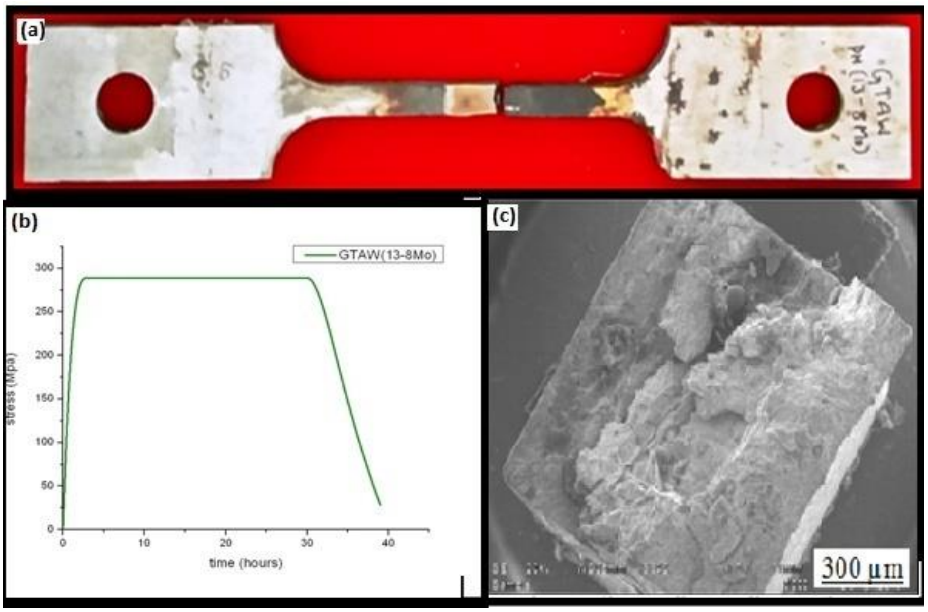

Fig. 17 Stress corrosion cracking specimen of PH 13-8 Mo GTA welds of high nitrogen stainless steel (a) failed SCC specimen (b) stress-time curve and (c) SEM fractograph

Table 5 Stress corrosion cracking testing data of gas tungsten arc welds of high nitrogen stainless steel

Material	Applied Stress (50% Y.S)	Environment	Failure location	Time to Failure, t_f
HNS	595 MPa	45% $MgCl_2$	Centre	25 Hours
11-10PH	238 MPa	45% $MgCl_2$	Weld interface	16 Hours
MDN 250	322 MPa	45% $MgCl_2$	Weld interface	33 Hours
13-8Mo	288 MPa	45% $MgCl_2$	HAZ	41 Hours

SCC failed test specimen of MDN 250 GTA weld is shown in Fig. 16a and stress-time curve is given in Fig. 16b. Failure time is found to be 33 hours. SEM fractograph as shown in Fig. 16c clearly gave evidence for multiple cracks in both the either sides of the weld interface for MDN 250 GTA welds. Failed test specimen of PH 13-8 Mo GTA welds is shown in Fig. 17a and stress-time curve is given in Fig. 17b. Failure time is found to be 41 hours. Weld interface attack near to heat affected zone region is observed. It may be due to lower pitting potential which may be prone to initiation of pits and selective dissolution of this region. SCC behavior depends on the chemical composition, microstructure, environment and testing methods. Weld interface regions were attacked due to variation in microstructure, chemical composition and relatively lower pitting potentials. The pitting corrosion and stress corrosion cracking resistance of high nitrogen stainless steel GTA welds is affected by the filler metal composition and found to be sensitive to microstructure. Hence, PH 13-8 Mo GTA welds resulted in favorable

microstructure and having better stress corrosion cracking resistance when compared to that of 11-10 PH and MDN 250 GTA welds in boiling 45% $MgCl_2$ solution.

4. Conclusions

1. Microstructure of nickel free high nitrogen stainless steel (HNS) consisted of fine grained austenite matrix. Presence of nitrogen has improved strength, ductility and toughness along with superior corrosion resistance.
2. Filler metal composition affects the microstructural morphology which in turn effects the pitting corrosion and stress corrosion cracking behaviour of high nitrogen steel welds.
3. Gas tungsten arc welds of nickel free high nitrogen steel resulted in formation of delta ferrite in the austenite matrix in the weld metal of 11-10PH and PH13-8Mo fillers. Reverted austenite in the martensite matrix was observed in weld zone of the MDN 250 filler.
4. Weld interface of 11-10 PH GTA weld was found to be having microporosity and is due to the presence of nickel which is having low solubility of nitrogen in the weld metal. Formation of unmixed zone near the fusion boundary was observed in weld interface of MDN 250 GTA welds.The weld interface of PH 13-8 Mo GTA welds is free from porosity and unmixed zone when compared to that of 11-10 PH and MDN 250 GTA welds.
4. Overall study established that GTA welds made with PH 13-8 Mo filler resulted in favorable microstructural changes and achieved better combination of mechanical properties and corrosion resistance when compared to GTA welds made with 11-10 PH ad MDN 250 fillers.

References

[1] R.P. Reed, Journal of Metals, 3, 1989, pp. 16-21.
[2] M.O. Speidel, Proc. Int. Conf. High-Nitrogen Steels, HNS 88, 1989, pp. 92.
[3] M.L. Byrnes, M. Grujicic, W.S. Owen, Acta Metall. 35, 7, 1987, pp. 1853-1862.
[4] J. Menzel, G. Stein, P. Dahlmann, Proc. Int. Conf. High-Nitrogen Steels, HNS 88, , 1989, pp. 147
[5] J.C. Rawers, J.S. Dunning, G. Asai, R.P. Reed, Metallurgical Transaction – A, 23A, 1992, pp. 2061.
[6.] J.C. Rawers, G. Asai, R. Doan, J.S. Dunning, Journal of Materials Research, 7, 1992, pp. 1083.
[7]M.O.Speidel, Uggowitzer P.J., Stickstofflegierte Stahle, Ergebnisse der Werkstoff Forschung Band 4, Thubal-Kain, Zurich, 1991.
[8] M.L.G. Byrnes, M. Grujicic and W.S. Owen, Acta Metalurgica, 35, 1987, pp. 1853.
[9] E. Werner, Material Science Engineering A, 101, 1988, pp. 93.
[10] M.DuToitandP.C.Pistorius, Welding Journal,2003, pp. 219-222.
[11] Woo Insuand Kikuchi Yasushi,Trans. JWRI,31, 2, 2002, pp. 129.
[12]MrityunjoyHazra, Kotipalli SrinivasaRao, Gankidi MadhusudhanReddy, Journal of Materials Research and Technology, 2014, pp. 90.
[13] Baldev Raj, P.Shankar and T Jayakumar, Advances in Stainless Steel, 2010, pp. 342.
[14] D.J. Kotecki, T.A. Sievert, Welding Journal, 1992, pp. 171-178.
[15] Madeleine du toit, Journal of materials engineering and performance. 11, 2002, pp. 312.
[16] Mohd Talha, C.K. Behera and O.P.Sinha, Journal of material science engineering C, 7, 2013, pp. 3563-3575.
[17] M.D Mathew and V.S. Srinivasan, Mechanical properties of nitrogen bearing steels, 2006, pp. 182.
[18] Speidel M.O, proc. of International conf. on high nitrogen steels, HNS 88,1989, pp. 92.
[19] U. Kamachi Mudali, R.K. Dayal, J.B. Gnanamoorthy and P. Rodriguez, Material Transactions, JIM, 37, 1996, pp. 1568-1573.
[20] O. Kamiya, Z.W. Chen and Y. Kikuchi, Journal of material science, 37, 2002, pp. 2475 – 2481.

[21] P. Venkata Ramana, G. Madhusudhan Reddy, T. Mohandas and A.V.S.S.K.S Gupta, Materials and Design, 31, 2010, pp. 749-760.
[22] O. Kamiya, Z.W. Chen and Y. Kikuchi, Journal of material science, 37, 2002, pp. 2475 – 2481.
[23] H. Shaikh, T. Anita, A. Poonouzhall, R.K. Dayal and B. Raj, woodhead publishing limited, 2011, pp. 427-482.

Acknowledgements
The authors would like to thank Director, Defence Metallurgical Research Laboratory Hyderabad, India for his continued encouragement and permission to publish this work.